

## Computer-simulation study of the phase diagram of the CH<sub>4</sub> monolayer on graphite: Corrugation effects

Hye-Young Kim and W. A. Steele

*Chemistry Department, Pennsylvania State University, University Park, Pennsylvania 16802*

(Received 13 May 1991; revised manuscript received 28 October 1991)

Molecular-dynamics simulation studies have been carried out for the two-dimensional phases of submonolayer methane physisorbed on graphite. Three methane-solid interaction potentials were used that differed by the size of the corrugation term in the molecule-solid potential function. Thermodynamic quantities were estimated throughout the commensurate-incommensurate and the melting transitions, and their dependence on the corrugation magnitude  $s$  was determined. Simulations with a corrugation magnitude 50% larger than that given by the pairwise spherical-site summation approximation to the potential give good agreement with experimental data.

### I. INTRODUCTION

The physisorption of small molecules on graphite has received considerable experimental and theoretical attention. Despite this, however, the understanding of the static and dynamic nature of physisorbed molecular films remains incomplete. Also, the known values of interactions of molecules in these systems are still not quantitatively satisfactory. Especially the search for the right value of the magnitude of the periodic variation in the molecule-solid holding potential (briefly, the corrugation) is actively going on. The observed phases formed in a physisorbed monolayer often suggest a higher corrugation than was originally obtained in calculations based on a pairwise summation of spherically symmetric site-site potentials.<sup>1</sup> In this study we will investigate the thermodynamic properties and the phase transitions of methane molecules adsorbed on graphite by molecular-dynamics computer simulation. The simulations were performed using three different values of corrugation:  $s=0$ , the flat substrate;  $s=1$ , as predicted by Steele;<sup>2</sup> and  $s=1.5$ . The results of the three sets of simulations will be compared with each other and with available experimental data.

The work presented here deals with methane on the graphite basal plane with coverage slightly smaller than that of a complete  $\sqrt{3}\times\sqrt{3}$  commensurate monolayer. This system, however, may be considered as a Lennard-Jones submonolayer since the interactions of methane molecules are here represented by Lennard-Jones (LJ) potentials. The structure and phase behavior of submonolayer methane adsorbed on graphite has been characterized by experimental studies of adsorption isotherm measurements<sup>3,4</sup> and by neutron scattering.<sup>5</sup> At low temperatures, the submonolayer was observed to be a  $\sqrt{3}\times\sqrt{3}$  commensurate solid (CS) phase. A continuous commensurate-incommensurate transition (CIT) to the expanded solid (ES) phase is found to occur near 50 K. Melting of methane on graphite occurs always from the ES phase. The melting transition is first order and takes place at a triple point just below 60 K in the submonolayer region. The transition temperature shifts upwards

with increasing surface coverage in the near-monolayer-completion region. Specifically, heat-capacity experiments by Marx and Wassermann<sup>3</sup> found two heat-capacity peaks, a broad weak anomaly at 47.6 K corresponding to CIT and a prominent peak at 56.2 K corresponding to the melting transition. More recently, Kim, Zhang, and Chan<sup>4</sup> conducted a heat-capacity experiment and also found a broad peak near 47 K and a  $\delta$ -function-like peak near 57 K. The structural changes indicated above for these transitions were confirmed by diffraction measurements.

In theoretical work, an anharmonic finite-temperature calculation<sup>6,7</sup> gave a temperature-driven CIT of first order at 41 K (or 44 K) and the ES was predicted to be a free-floating two-dimensional solid without domain walls.

In this paper, we will present the results of constant-temperature molecular-dynamics (MD) simulations carried out at a surface coverage of  $n=0.8$  monolayer, with the monolayer defined to be a  $\sqrt{3}\times\sqrt{3}$  commensurate phase.

The interaction potentials used in this study are introduced in Sec. II, and the details of calculations are described in Sec. III. The results are discussed in Sec. IV and summarized in Sec. V.

### II. INTERACTION POTENTIAL

In this study methane is considered as a spherical molecule. This is a reasonable assumption for the temperature range in our study since earlier studies showed that above 20–30 K, methane molecules on graphite are undergoing rapid rotational diffusion.<sup>8,9</sup>

The interaction potential used in this study is composed of two parts: gas-gas and gas-surface interactions. For the gas-gas interaction ( $V_{gg}$ ), a LJ 12-6 intermolecular potential is used with two-dimensional parameters  $\epsilon_{gg}^{2D}$  and  $\sigma_{gg}^{2D}$  modified from bulk values ( $\epsilon_{gg}^{3D}$  and  $\sigma_{gg}^{3D}$ ) to include the substrate-mediated interaction ( $\Delta V_M$ ).

$$V_{gg}(r) = V_{gg}^{3D}(r) + \Delta V_M(r) \quad (1)$$

$$= 4\epsilon_{gg}^{2D} \left[ \left( \frac{\sigma_{gg}^{2D}}{r} \right)^{12} - \left( \frac{\sigma_{gg}^{2D}}{r} \right)^6 \right]. \quad (2)$$

LJ parameters for bulk methane molecules are quite well known and we have adopted the values of  $\epsilon_{gg}^{3D}/k_B = 148.2$  K and  $\sigma_{gg}^{3D} = 3.817$  Å.<sup>10,11</sup> ( $\epsilon_{gg}^{3D}$  is the reduced unit of energy throughout the present work unless specified otherwise.) The substrate-mediated change in the pairwise potentials for a physisorbed adlayer has been recognized to play an important role.<sup>12-16</sup> The two largest of these are the McLachlan interaction and the triple-dipole dispersion interaction. Kim and Cole<sup>16</sup> have found that the relatively small contribution of triple-dipole dispersion interaction may be included effectively into the McLachlan expression<sup>17</sup> if the adatom height  $L$  was referred to an effective image plane at  $z_0 = 1$  Å above the outermost carbon atoms on the graphite basal plane. When two particles lie in a common plane, a distance  $L$  ( $=z - z_0$ ) above the interface, McLachlan's result<sup>17</sup> is

$$\Delta V_M(\rho) = \frac{4C_{s1}}{(\rho R)^3} \left[ \frac{1}{3} - \frac{L^2}{R^2} \right] - \frac{C_{s2}}{R^6}, \quad (3)$$

$$R^2 \equiv \rho^2 + 4L^2. \quad (4)$$

Here,  $\rho$  is the lateral separation between two adsorbed particles. The coefficients  $C_{s1}$  and  $C_{s2}$  have been determined for many absorption systems<sup>12,18-20</sup> and formulas exist for the general case.<sup>21</sup> In the present study, these substrate-mediated interactions are effectively included in the intermolecular LJ 12-6 potential by reducing the well depth  $\epsilon_{gg}^{3D}$  by 8% and increasing  $\sigma_{gg}^{3D}$  by 0.02 Å whenever both molecules are in the first adsorbed layer: thus,  $\epsilon_{gg}^{2D}/k_B = 136.3$  K and  $\sigma_{gg}^{2D} = 3.837$  Å.

The gas-surface potential ( $V_{gs}$ ) is based on a LJ pair potential between methane and carbon sites.<sup>2</sup> The parameters were based on an analysis of experimental studies of the properties of methane on graphite at high temperature;<sup>22</sup> values used are  $\epsilon_{gs}/k_B = 66$  K and  $\sigma_{gs} = 3.6$  Å. The summation over the atoms in the solid was transformed into the two-dimensional Fourier-series expansion for gas-surface interaction introduced by Steele:<sup>2</sup>

$$V_{gs}(\mathbf{r}) = V_{gs0}(z) + \sum_{n>0} V_{gsn}(z) f_n(x, y). \quad (5)$$

In the present study, the laterally averaged part is written in the Euler-MacLaurin form and only the first set of Fourier component terms reflecting the two-dimensional periodicity of the substrate are retained:

$$V_{gs0}(z) = \frac{8\pi\epsilon_{gs}\sigma_{gs}^6}{\sqrt{3}a_0^2} \left[ \frac{2\sigma_{gs}^6}{5z^{10}} + \frac{2\sigma_{gs}^6}{45d(z+0.72d)^9} - \frac{1}{z^4} - \frac{2z^2+7dz+7d^2}{6d(z+d)^5} \right], \quad (6)$$

$$V_{gs1}(z) = \frac{4\pi\epsilon_{gs}\sigma_{gs}^6}{\sqrt{3}a_0^2} \left[ \frac{\sigma_{gs}^6}{30} \left[ \frac{2\pi}{\sqrt{3}a_0z} \right]^5 K_5 \left[ \frac{4\pi z}{\sqrt{3}a_0} \right] - 2 \left[ \frac{2\pi}{\sqrt{3}a_0z} \right]^2 K_2 \left[ \frac{4\pi z}{\sqrt{3}a_0} \right] \right], \quad (7)$$

$$f_1(x, y) = -2 \left[ \cos \frac{2\pi}{a_0} \left[ x + \frac{y}{\sqrt{3}} \right] + \cos \frac{2\pi}{a_0} \left[ x - \frac{y}{\sqrt{3}} \right] + \cos \frac{4\pi}{\sqrt{3}a_0} y \right]. \quad (8)$$

Here,  $d(=3.4$  Å) is the interlayer spacing of graphite and  $K_n$  is the modified Bessel function of the second order.  $a_0(=2.46$  Å) is the reduced unit of length used throughout the present work. The multiplicative factor in this first Fourier component term ( $V_{gs1}$ ), reflecting the corrugation of the substrate, has been a subject of many studies on its own. The observed phases formed in physisorbed monolayer often suggest a much higher corrugation than that given by Eq. (7), which is based on spherical LJ pair potentials between the adatom and each carbon site.<sup>1,2</sup> Vidali and Cole<sup>1</sup> calculated  $V_{gs1}$  from a direct summation of two-body anisotropic interaction of an adatom-carbon site taking into account the graphite anisotropy and suggested  $V_{gs1}$  of the order of twice the value computed by Steele.<sup>2</sup> Kim and Cole<sup>23</sup> calculated the anisotropic three-body contribution, involving sets of an adatom and two carbon atoms, to  $V_{gs1}$  and found that this term tends to reduce the corrugation. In the present study, Eq. (5) is modified to read

$$V_{gs}(\mathbf{r}) = V_{gs0}(z) + sV_{gs1}(z)f_1(x, y). \quad (9)$$

Thus,  $s=1$  corresponds to corrugation as originally computed by Steele<sup>2</sup> and  $s=1.5$  gives a more corrugated surface within the range suggested by Cole and co-workers.<sup>1,23</sup>

### III. CALCULATION

Throughout the present study, molecular dynamics are employed using the isokinetic constraint method<sup>24-26</sup> in the fifth-order Gear predictor-corrector algorithm and link-cell technique. This constraint method is known to generate correct configurational properties in the canonical ensemble.<sup>27,28</sup> In the link-cell technique, the simulation box containing 289 molecules ( $N$ ) is divided into 64 cells and a particular molecule in a cell may interact with molecules in the same cell and also with the molecules in the first- and second-nearest-neighboring cells. This truncates the pair interaction potentials at about 18 Å; there are no corrections made for interactions beyond this range.

The simulation box size was taken to be  $(30 \times 18\sqrt{3})a_0^2$ . Thus, the number density of this system corresponds to 0.8 commensurate monolayer. Periodic boundary conditions are imposed in both  $x$  and  $y$  directions and a reflecting wall is placed at the height of 34 Å above the surface. (In the present study, due to the relatively low coverage and temperature, molecules never leave the first

adsorbed layer.) Each time step corresponds to 0.0022 ps.

Three series of calculations are performed: 10, 53, 54, and 55 K for  $s=0$ ; 10, 45, 47, 49, 51, 53, 55, 56, 57, and 59 K for  $s=1$ ; and 10, 31, 35, 39, 45, 47, 48, 49, 50, 51, 53, 55, 56, 57, 59, 61, and 63 K for  $s=1.5$ . Most calculations are conducted in heating curves where the simulation for one temperature is started from a configuration of a neighboring lower-temperature run. At the start of some calculations the system consisted of a perfect rectangular patch of molecules in an (unregistered) triangular lattice configuration. Equilibration was achieved during 5000 time steps by zeroing out the total momentum of the system and scaling velocities to the desired temperature in each time step. Then the system is relaxed for at least another 5000 (dead) time steps without resetting the total momentum or scaling velocities. At temperatures away from the melting temperature, 10 000 time steps (22 ps) at least and very near the transition, 640 000 time steps (1.4 ns) at most are performed. The positions and velocities of particles are saved every 40 to 80 time steps. Properties calculated include averages of the component molecule-solid and molecule-molecule energies, heat capacities, mean-squared displacements, velocity autocorrelation functions, pair-correlation functions, one-dimensional density distribution functions, and the misfit between the methane and the graphite lattice spacing.

#### IV. RESULTS

The density profile of the molecules as a function of height above the surface given in Fig. 1 shows that the amplitude of vibration perpendicular to the surface increases significantly with increasing temperature even though the molecules remain bound to the surface for all temperatures considered. This result shows that the tran-

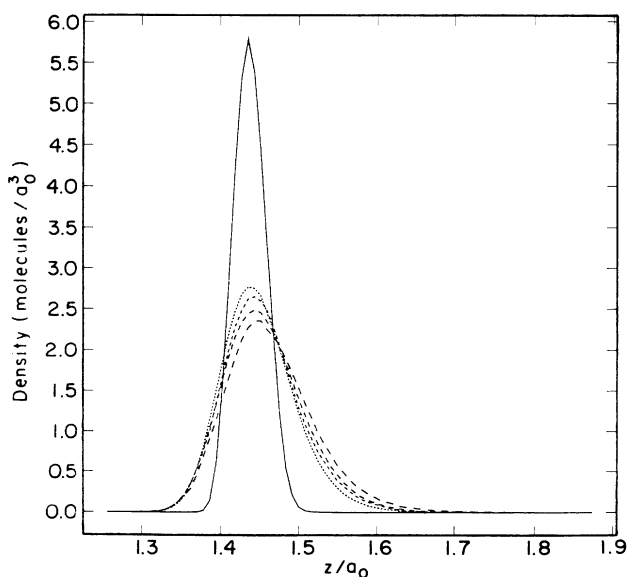


FIG. 1. Local densities for  $s=1.5$  plotted as a function of the distance  $z$  away from the graphite surface. At the peaks, they are 10, 45, 50, 55, and 63 K, from the top down.

sitions of these methane monolayers are primarily two-dimensional. This one-dimensional density distribution function shows a continuous shift of peak position from 3.55 Å (10 K) to 3.59 Å (59 K) for  $s=1$  and 3.53 Å (10 K) to 3.57 Å (63 K) for  $s=1.5$ . For a flat substrate,  $s=0$ , an equilibrium height  $z_{eq}$  is found at 3.51 Å in the solid (53 and 54 K) and at 3.55 Å in the liquid phase (55 K).

At low temperature, the methane submonolayer adsorbed on graphite is experimentally observed to be in a  $\sqrt{3} \times \sqrt{3}$  commensurate solid phase,<sup>5</sup> where molecules form a triangular lattice with commensurate lattice spacing  $d_c = \sqrt{3}a_0$ . Our low-temperature simulations at 10 K found a triangular lattice with lattice spacing  $d = 1.747a_0$ ,  $1.736a_0$ , and  $1.735a_0$  for  $s=0$ , 1, and 1.5, respectively. Thus, the corrugated substrates, both  $s=1$  and 1.5, give lattice spacing quite close to that of a commensurate solid with a small misfit of  $-0.2\%$  while flat substrate,  $s=0$ , gives a little larger misfit of  $-0.9\%$ . At all temperatures, misfits  $M$  of lattice spacing ( $d$ ) are obtained from the evaluations of running averages of the square root of the Voronoi hexagon area ( $A$ ) per molecule in a solid patch;

$$M(\%) = \left[ 1 - \frac{d}{d_c} \right] 100, \quad d_c = \sqrt{3}a_0, \quad (10)$$

$$= \left[ 1 - \left[ \frac{A}{A_c} \right]^{1/2} \right] 100, \quad A_c = \frac{3\sqrt{3}a_0^2}{2}. \quad (11)$$

The Voronoi polygon, the generalization of the Wigner-Seitz cell, is a convex polygon enclosing a particle  $i$  with sets of points closer to particle  $i$  than to any other particle. Thus the area of a polygon corresponds to the area occupied by a particle enclosed in it. Also a particle having Voronoi polygons of  $m$  sides has  $m$  neighbors. The triangular lattice solid patch mostly consists of Voronoi hexagons with some exceptions for the particles on the edges of the patch. Edge particles are excluded in the misfit calculation by considering only the Voronoi hexagons. The small misfits found in the 10 K simulations for both corrugated substrates are in satisfactory agreement with experimental observation of commensurate solid at low temperature and density.

Averages of the components of the methane energy at 10 K are listed in Table I for all three corrugations. Considering the estimated uncertainty of 0.01 in each of these values, the changes with  $s$  are almost insignificant except for the average molecule-solid corrugation energy. Here, the change is nearly linear in  $s$ . (A quadratic dependence was predicted by Monson, Steele, and Henderson<sup>29</sup> in their perturbation treatment of this term.)

TABLE I. Components of the average interaction energy per molecule at 10 K (units are reduced by dividing by  $\epsilon_{gg}^{3D}$ , with  $\epsilon_{gg}^{3D}/k_B = 148.2$  K).

$s$	0	1	1.5
$\bar{V}_{gg}/N$	-2.77	-2.78	-2.78
$\bar{V}_{gs0}/N$	-9.58	-9.56	-9.54
$\bar{V}_{gs1}/N$	0	-0.17	-0.28
$\bar{V}_{tot}/N$	-12.35	-12.51	-12.60

As mentioned in the Introduction, the effect of substrate corrugation on the phase diagram of the methane (Lennard-Jones system in general) submonolayer on graphite is the main interest here. The  $s=0$  2D system has been a subject of many intensive studies which provides a comparison with our system. The trajectory plots shown in Fig. 2 for the molecules in the adsorbed layer with  $s=0$  clearly demonstrate a crystal phase at  $T^*=0.396$  ( $T=54$  K) and a liquid phase at  $T^*=0.403$  ( $T=55$  K). Here,  $T^* \equiv k_B T / \epsilon_{gg}^{2D}$ . The latent heat of melting of  $l_m^* = 0.24 \pm 0.06$  is estimated from the difference of the total potential energies per molecule in solid (55 K) and liquid (54 K) phases. Our estimate of the triple point temperature  $T_t^* = 0.400 \pm 0.004$  is in excellent agreement with the value  $T_t^* = 0.40 \pm 0.01$  obtained by Phillips, Bruch, and Murphy<sup>30</sup> and is slightly lower than the value  $T_t^* = 0.415$  given by Barker, Henderson, and Abraham<sup>31</sup> and by Abraham.<sup>32,33</sup> Within the combined uncertainties the latent heat of melting agrees with the value  $l_m^* = 0.27 \pm 0.05$  obtained at  $T_t^* = 0.40 \pm 0.01$  by Phillips, Bruch, and Murphy.<sup>30</sup> In summary, our system produces satisfactory results for a Lennard-Jones submonolayer on a flat substrate and is consistent with first-order melting at a melting temperature between 54 and 55 K for methane submonolayer on graphite. We emphasize that the LJ melting parameters reported by other workers are for strictly 2D systems. Although perturbation theory has been used to estimate the effects of motion perpendicular to the surface upon an otherwise 2D system,<sup>34</sup> it is not clear that this motion will produce a significant change in the melting character of monolayer films on graphite.

In the absence of an accurate *a priori* estimate of the corrugation for the methane submonolayer on real graphite, we have chosen two reasonable values of corrugation parameters ( $s=1$  and 1.5) to study the effects of corrugation on the observables of this system.

The temperature dependencies of the energetics of the monolayer are shown in Fig. 3 for both  $s=1$  and 1.5. Both corrugation values give quite similar trends in the various components of energies. For both  $s$  values, the change in the term representing the laterally averaged gas-surface potential per molecule ( $V_{gs0}/N$ ) is effectively linear over the entire temperature range, with a slope of  $0.5k_B$  per particle as expected for a one-dimensional har-

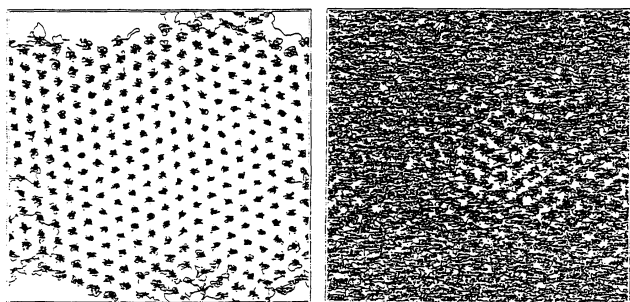


FIG. 2. Trajectory plots for  $s=0$  at 54 and 55 K. The elapsed time is 44 and 88 ps, respectively.

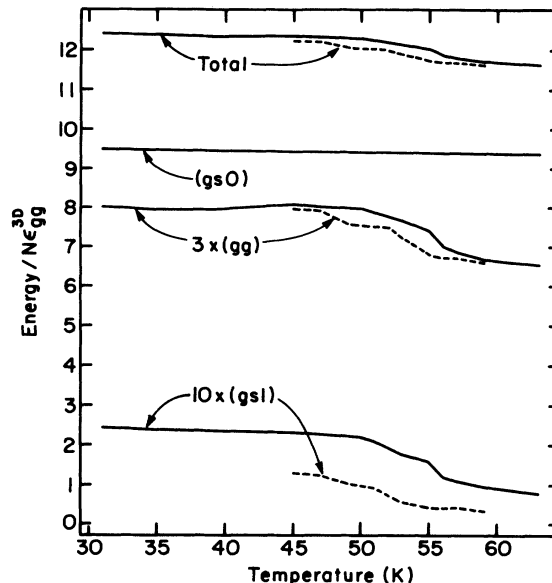


FIG. 3. Energies per molecule for  $s=1$  (dashed curve) and  $s=1.5$  (solid curve): total potential energy  $V_{tot}/N$ , gas-gas energy  $V_{gg}/N$ , the laterally averaged term ( $V_{gs0}/N$ ), and the corrugation term ( $V_{gs1}/N$ ) of the gas-surface potential energy. The laterally averaged terms for both  $s$  values are identical.

monic oscillator. The other component energies, the gas-gas ( $V_{gg}/N$ ), and the corrugation contribution to gas-surface ( $V_{gs1}/N$ ), show temperature-dependent slopes. These changes correspond to the peaks in the residual heat capacity shown in Fig. 4. (The residual heat capacities are obtained from the fluctuations of the total potential energies as a function of time, not from the change of total potential energy as a function of tempera-

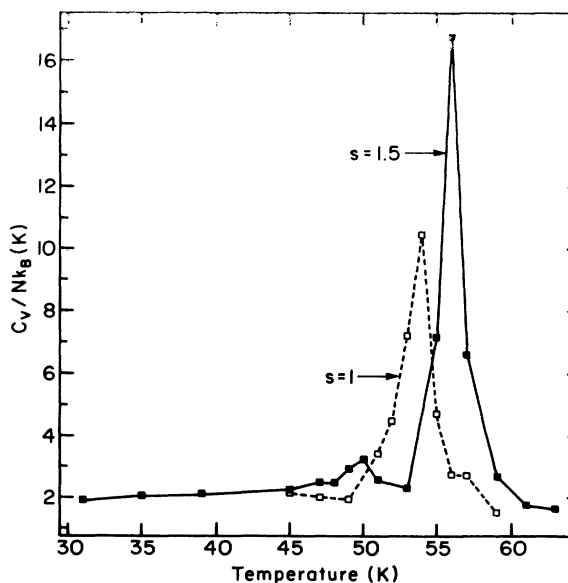


FIG. 4. Residual heat capacity for  $s=1$  (open squares) and  $s=1.5$  (solid squares). Curves are drawn as a guide to the eye.

ture. To obtain the molar heat capacity due to the fluctuations of the total energy, one adds the  $1.5R$  due to kinetic-energy fluctuations.) As is well known, the thermodynamic and structural properties produced by simulations of a small system with periodic boundary conditions are affected by finite-size effects that make it almost impossible to observe a first-order thermodynamic transition. However, the properties of this simulation system exhibit sharp changes near melting which are generally supportive of the experimental determination of a first-order transition in this system. Of course, the simulations produce microscopic information which is unavailable to the experimentalist. For example, one can plot the computer-generated trajectories followed by the molecules over periods of up to 88 ps. Four such plots for  $s=1.5$  at 56 K are shown in Fig. 5. Here, regions where vibrational motion is occurring are quite distinct from the areas where the chaotic trajectories that characterize a liquid may be seen. For such a small system, two-phase coexistence in the classical sense is not expected, but certainly these fluctuating (in time) regions exhibit distinctly solidlike and liquidlike motions. The existence of extensive boundaries between the two types of regions makes it difficult to split the system into areas with two (and only two) densities and energies, but simulations are now underway using much larger samples in this "coexistence" region in an attempt to resolve this question.

If a heat of melting is defined as a difference of the total potential energies per molecule at temperatures just above and below the melting temperature, the simulations yield approximately 25 and 35 K for  $s=1$  and 1.5, respectively, which are in good agreement with 30 K observed in the thermodynamic experiment by Kim, Zhang, and Chan.<sup>4</sup> The melting temperature of  $56 \pm 1$  K for

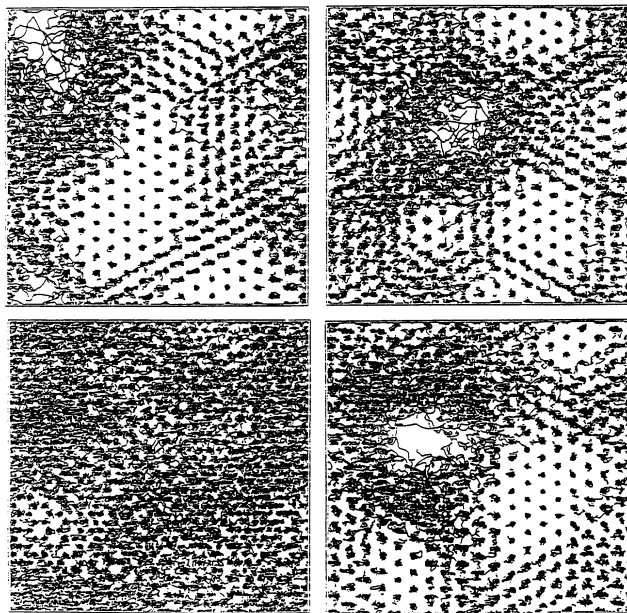


FIG. 5. Four trajectory plots at 56 K for  $s=1.5$ : each trajectory plot has an elapsed time of 88 ps and is selected 132 ps apart.

$s=1.5$  agrees very well with the experimental observations<sup>3,4</sup> and is higher than those of  $54 \pm 1$  K for the two smaller  $s$  values.

The melting transition can also be seen from the values of the adatom mobility in the plane parallel to the surface. The mobility, shown in Fig. 6, is obtained from the slope of the molecular mean-square displacements as a function of time. To avoid any contribution from drifting edge particles, only particles with at least three neighbors (in Voronoi polygon construction) are considered when the layer is solid while all the particles are considered in the liquid phase. (In the liquid phase, thermal expansion causes the whole surface to be covered with particles with the possible exception of a small hole.) In Fig. 6, the mobilities for all three  $s$  values,  $s=0$ , 1, and 1.5, are shown. The flat substrate results show a very sharp increase of mobility at the melting temperature while the corrugated substrate results show a slow increase of mobility even below the melting temperature and a large jump to a higher mobility at the melting temperature. The slow increase of mobility below the melting temperature seems to be due to the particles involved in a domain-wall structure observed in the incommensurate solid phase.

2D pair-correlation functions  $g(r)$  for  $s=1.5$  were calculated during the simulations and are given in Fig. 7. Significant changes in  $g(r)$  are observed as the temperature increases from 50 to 56 K, most noticeably in the second and third peaks. At temperatures lower than 50 K, the second peak is higher than the third one. After 50 K, the heights of second and third peaks become nearly the same and the peak positions shift outward, indicating that the solid phase system is expanding. At 56 K, the third peak becomes higher than the second one and as temperature further increases the peaks are rapidly broadened, indicating that the system is in a liquid

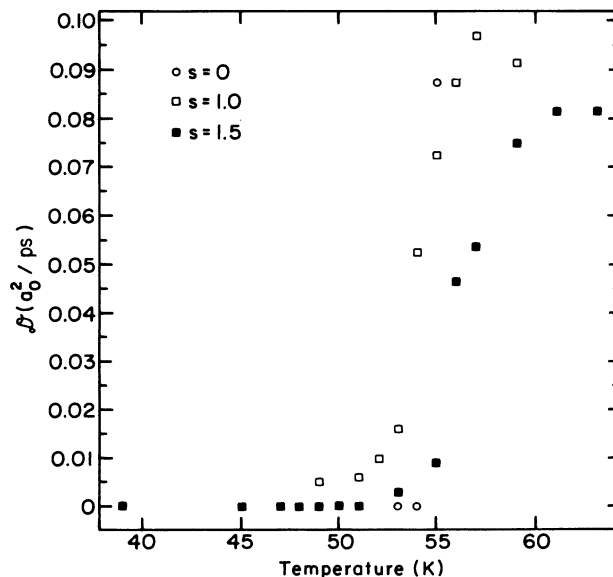


FIG. 6. In-plane diffusion constants for  $s=0$  (open circles),  $s=1$  (open squares), and  $s=1.5$  (solid squares).

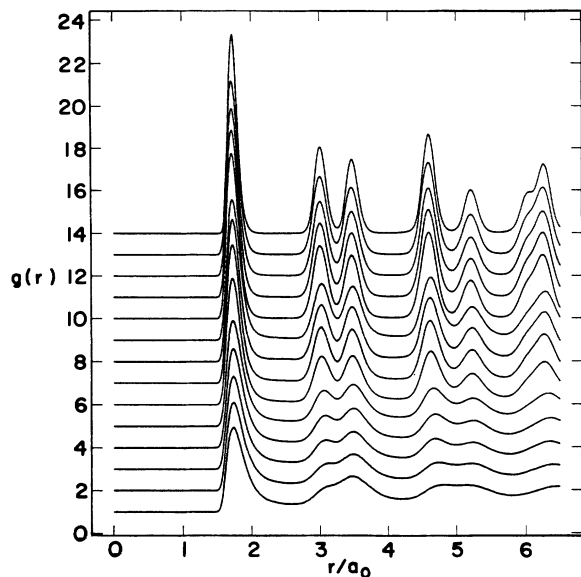


FIG. 7. Pair-correlation function  $g(r)$  for  $s=1.5$  at various temperatures; from the top down, they are 31, 35, 39, 45, 49, 50, 51, 53, 55, 56, 57, 59, 61, and 63 K. Curves for different temperatures are displaced vertically.

phase.

For  $s=1.5$ , the data plotted in Fig. 4 show a small peak in the heat capacity at 50 K in addition to the large peak at 56 K corresponding to melting. For  $s=1$  no such structure is observed. This first peak at 50 K has indeed been observed near 47 K in the thermodynamics experiments<sup>3,4</sup> and referred to as CIT. Some indications of this CIT at 50 K also appear in other simulated observables for  $s=1.5$ : slope changes in the energies (Fig. 3), slow increase of mobilities before melting (Fig. 6), and changes in the shape of peaks in the pair-correlation function (Fig. 7).

To investigate the CIT region, the misfits of lattice spacing are obtained in the way described earlier. These data are presented in Fig. 8 for all three values of  $s$ . The misfits at 10 K have already been discussed. For the flat substrate ( $s=0$ ), it is hard to tell the trends due to an insufficient number of simulations, other than the fact that the misfits increase up to  $-4.7\%$  at 54 K before the system melts. From trajectory plots, however, we find that the solid phase is a simple patch which shows the expected continuous increase in lattice spacing. On the other hand, for the corrugated substrates (both  $s=1$  and  $1.5$ ), there are sudden slope changes in the misfits at 49 K ( $s=1$ ) and 51 K ( $s=1.5$ ) as temperature increases. Until that temperature the misfits change quite slowly up to  $-1.0\%$  at 47 K and  $-0.7\%$  at 50 K for  $s=1$  and  $1.5$ , respectively. After that, the misfits change up to  $-5.5\%$  at 53 K for  $s=1$  and  $-3.3\%$  at 55 K for  $s=1.5$  before the system melts. Although slope change is clear for both nonzero  $s$  values, there is no small peak in the residual heat capacity for  $s=1$  as is for  $s=1.5$ . It is possible that the peak is too small to be detected in our temperature intervals. For  $s=1.5$ , on the other hand, the sudden misfit slope change occurs at the same temperature where the

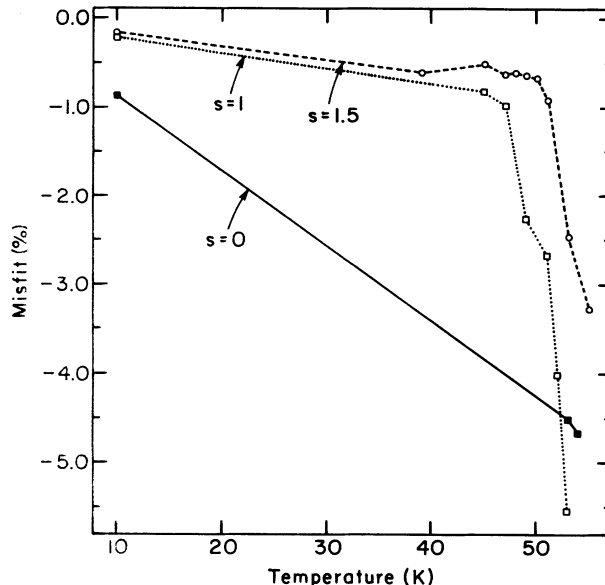


FIG. 8. Misfit (%) between the solid methane and the commensurate lattice spacing for  $s=0$  (solid squares),  $s=1$  (open squares), and  $s=1.5$  (open circles). Curves are guides to the eye.

small heat-capacity peak occurs.

Excellent reviews of the properties of the incommensurate monolayer are provided elsewhere.<sup>35-37</sup> The general idea is that the substrate can induce density modulations in the monolayer which occur on length scales much larger than the interatomic distances. For physisorbed gases on graphite, the adsorption sites are at the centers of the hexagons and are spaced  $a_0$  apart. At densities where the monolayer is close to being commensurate, large patches of adatoms are in fact registered in  $\sqrt{3} \times \sqrt{3}$  sublattices based on the three possible centers. These patches (or domains) are separated from each other by domain walls, at which the densities of the monolayer varies significantly from commensurate. Since free-space lattice spacing of methane molecules is larger than  $\sqrt{3}a_0$ , the densities at the domain walls will be less than those of commensurate domains.

Domain structure can be found in the trajectory plots for both nonzero  $s$  values. At low temperatures, these systems consist in large solid patches with few drifting edge particles and no domain walls. As the temperature increases, one or two very unstable small domain walls start to show up briefly in the corner of the patch during simulations. More stable but quite mobile domain walls form with an increasing number of domains up to about four as temperature approaches the melting temperatures. As an example, trajectory plots (88 ps each) at four temperatures for  $s=1.5$  are presented in Fig. 9. As mentioned earlier, there are three distinct  $\sqrt{3} \times \sqrt{3}$  sublattices based on the three possible centers of the graphite hexagons. When these molecules are in a different center from that of the rest of the molecules, there exist two distinct domains separated by a domain wall. At 53 K, some molecules are shown to reside at two or even three centers during 88 ps making three distinct domains observable for different periods of time. As temperature in-

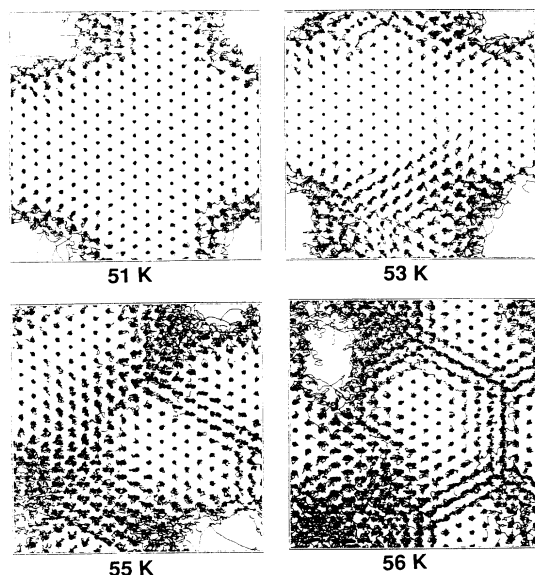


FIG. 9. Trajectory plots of the incommensurate solid phases (51, 53, 55, and 56 K) for  $s=1.5$ . Each trajectory plot has an elapsed time of 88 ps.

creases, more domains are observed. This increase of the number of domains in the CIT region was also observed in a simulation work of Suh, Lermer, and O'Shea<sup>38</sup> on the CIT of xenon submonolayer adsorbed on graphite. In their work they have used the corrugation of Steele ( $s=1$  here) and concluded that the experimentally observed increase of lattice spacing in CIT is due to the increasing number of domains (or number of particles composing the domain walls) in the solid patch. Our results are consistent with this conclusion.

The small increase of misfit observed in the lower-temperature range may be considered as a finite-size effect due to the fact that the particles near the edge of the commensurate solid patch are more relaxed than the particles in the middle of the patch. Our estimated misfit of  $-3.3\%$  for  $s=1.5$  before melting is a little larger than the experimentally observed value of  $\sim -1.6\%$  from the neutron-scattering experiment done by Vora, Sinha, and Crawford.<sup>5</sup> The estimated CIT transition temperature of 47 K for  $s=1$  and 50 K for  $s=1.5$  is in fair agreement with experimental data.<sup>3,4</sup>

As one might expect, the  $s=1$  case gives larger misfits than the  $s=1.5$  case for all the temperature ranges we studied; the smaller corrugation of substrate allows the system to expand more easily.

## V. DISCUSSION

We have used constant-area isothermal molecular-dynamics simulations to determine the corrugation effects on the observables of the submonolayer methane molecules. Many thermodynamic states were studied using three different corrugation values ( $s=0, 1$ , and  $1.5$ ). Overall, the  $s=1.5$  results were in the best agreement

with experimental data. Our simulations for the case  $s=0$  yield melting parameters in good agreement with other similar studies. Also, we find continuous commensurate-incommensurate transitions for both nonzero values of  $s$ .

It is well known that it is very difficult to distinguish between a first-order and a sharp but continuous phase transition in simulations of monolayer melting.<sup>39-41</sup> This problem is particularly difficult for small systems. Visually, the trajectory plots for temperatures near 56 K appear to show two-phase coexistence. Since one expects larger fluctuations near a phase transition, continuous or not, the appearance of the trajectories cannot be considered to be a proof. We have attempted to strengthen this argument by evaluating the distributions of methane-methane energy per particle in the films at various temperatures. Some of the results are shown in Fig. 10 for  $s=1.5$ . For temperatures ranging up to 55 K, this energy for a molecule in the solid has a peak at  $\sim -420$  K ( $\sim -70$  K per neighbor); small peaks are observed at  $\sim -280$  and  $\sim -210$  K which correspond to edge molecules having four and three neighbors, respectively. As temperature increases, the peaks in the histogram are increasingly broadened due to the effect of thermal motion upon the pairwise energies. At 55 K, the primary solid peak in the histogram is hardly shifted from its position at 48 K. In contrast, a single broad peak with a maximum at  $\sim -340$  K is found for the liquid at 61 K. However, histograms at 56 and 57 K show behavior best described as two overlapping peaks, one with its maximum close to that for the solid and the other close to that for the liquid. This is precisely the expected behavior for coexisting phases.<sup>39</sup> The fact that coexistence is present over a narrow interval of temperature is most

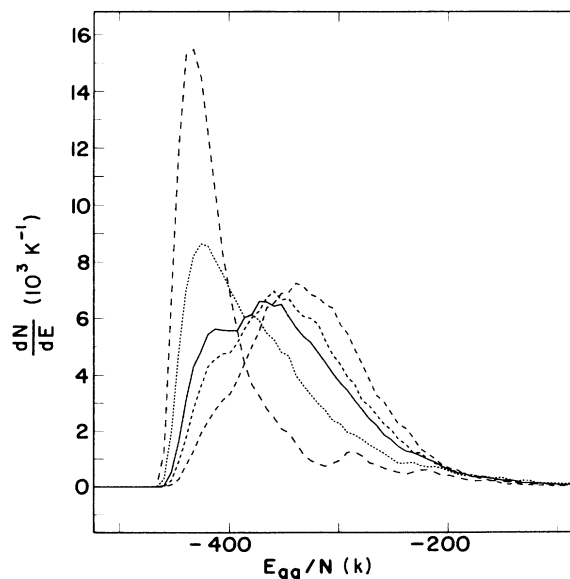


FIG. 10. Distribution of methane-methane interaction energies per molecule for  $s=1.5$  [48 K (long-dashed line), 55 K (dotted line), 56 K (solid line), 57 K (short-dashed line), 61 K (medium-dashed line)].

likely a finite-size effect.

It is observed that domain structure develops in the incommensurate solid for both cases with nonzero  $s$ . The thermodynamic changes in the 2D solid associated with these domain walls appear to produce some pretransitional changes that make it even more difficult to characterize the simulation melting as first order. In fact, it has recently been suggested that the primarily continuous nature of the melting of an argon monolayer on graphite is due to domain-wall melting in that incommensurate layer.<sup>42-44</sup> For methane, which exhibits a much smaller misfit than argon, the domains are larger (and the walls are regions of low density relative to the domains, in contrast to the argon monolayer). Although the computer sample of 289 molecules is too small to obtain much information about the domain-wall structure, the data

presented here are capable of giving a general picture, which is one of a sharp melting transition which exhibits pretransitional changes not seen for the  $s=0$  case. This conclusion is certainly consistent with experiments, but a stronger proof that first-order melting is present in the model system awaits results of current work on much larger samples in the immediate vicinity of the melting region.

#### ACKNOWLEDGMENTS

Instructive discussion on this subject with Dr. N. D. Shrimpton and useful correspondence with Professor M. H. W. Chan are gratefully acknowledged. This work was supported by Grant No. DMR-8718771 of the NSF.

- 
- <sup>1</sup>G. Vidali and M.W. Cole, *Phys. Rev. B* **29**, 6736 (1984).  
<sup>2</sup>W. A. Steele, *Surf. Sci.* **36**, 317 (1973).  
<sup>3</sup>R. Marx and E. F. Wassermann, *Surf. Sci.* **117**, 267 (1982).  
<sup>4</sup>H. K. Kim, Q. M. Zhang, and M. H. W. Chan, *Phys. Rev. B* **34**, 4699 (1986).  
<sup>5</sup>P. Vora, S. K. Sinha, and R. K. Crawford, *Phys. Rev. Lett.* **43**, 704 (1979).  
<sup>6</sup>J. M. Phillips, *Phys. Rev. B* **29**, 4821 (1984).  
<sup>7</sup>J. M. Phillips, *Phys. Rev. B* **29**, 5865 (1984).  
<sup>8</sup>P. Thorel, J. P. Coulomb, and M. Bienfait, *Surf. Sci.* **114**, L43 (1983).  
<sup>9</sup>M. W. Newbery, T. Rayment, M. V. Smalley, R. K. Thomas, and J. W. White, *Chem. Phys. Lett.* **59**, 461 (1978).  
<sup>10</sup>A. Michels and G. W. Nederbragt, *Physica* **2**, 1000 (1935).  
<sup>11</sup>J. R. Sams, *J. Chem. Phys.* **43**, 2243 (1965).  
<sup>12</sup>L. W. Bruch, *Surf. Sci.* **125**, 194 (1983).  
<sup>13</sup>L. W. Bruch and J. M. Phillips, *Surf. Sci.* **91**, 1 (1980).  
<sup>14</sup>J. Unguris, L. W. Bruch, E. R. Moog, and M. B. Webb, *Surf. Sci.* **109**, 522 (1981).  
<sup>15</sup>J. Unguris, L. W. Bruch, M. B. Webb, and J. M. Phillips, *Surf. Sci.* **114**, 219 (1984).  
<sup>16</sup>H.-Y. Kim and M. W. Cole, *Surf. Sci.* **194**, 257 (1988).  
<sup>17</sup>A. D. McLachlan, *Mol. Phys.* **7**, 381 (1964).  
<sup>18</sup>C. Schwartz and R. J. Le Roy, *Surf. Sci.* **166**, L141 (1986).  
<sup>19</sup>M. Karimi and G. Vidali, *Phys. Rev. B* **34**, 2794 (1986).  
<sup>20</sup>M. Karimi and G. Vidali, *Surf. Sci.* **191**, L799 (1987).  
<sup>21</sup>S. Rauber, J. R. Klein, M. W. Cole, and L. W. Bruch, *Surf. Sci.* **123**, 173 (1982).  
<sup>22</sup>M. J. Bojan, R. van Slooten, and W. A. Steele, *J. Sep. Sci. Technol.* (to be published).  
<sup>23</sup>H.-Y. Kim and M. W. Cole, *Phys. Rev. B* **35**, 3990 (1987).  
<sup>24</sup>M. P. Allen and D. J. Tildesley, *Computer Simulation of Liquids* (Oxford University Press, Oxford, 1987), p. 230.  
<sup>25</sup>W. G. Hoover, *A. Rev. Phys. Chem.* **34**, 103 (1983).  
<sup>26</sup>D. J. Evans and G. P. Morriss, *Comput. Phys. Rep* **1**, 297 (1984).  
<sup>27</sup>D. J. Evans and G. P. Morriss, *Phys. Lett.* **98A**, 433 (1983).  
<sup>28</sup>S. Nosé, *J. Chem. Phys.* **81**, 511 (1984).  
<sup>29</sup>P. A. Monson, W. A. Steele, and D. Henderson, *J. Chem. Phys.* **74**, 6431 (1981).  
<sup>30</sup>J. M. Phillips, L. W. Bruch, and R. D. Murphy, *J. Chem. Phys.* **75**, 5097 (1981).  
<sup>31</sup>J. A. Barker, D. Henderson, and F. F. Abraham, *Physica (Utrecht) A* **106**, 226 (1981).  
<sup>32</sup>F. F. Abraham, *Phys. Rep.* **80**, 339 (1981).  
<sup>33</sup>F. F. Abraham, *Adv. Phys.* **35**, 1 (1986).  
<sup>34</sup>P. A. Monson, M. W. Cole, F. Toigo, and W. A. Steele, *Surf. Sci.* **122**, 401 (1982).  
<sup>35</sup>P. Bak, *Rep. Prog. Phys.* **45**, 587 (1982).  
<sup>36</sup>V. L. Pokrovsky and A. L. Talapov, *Theory of Incommensurate Crystals* (Harwood Academic, New York, 1984).  
<sup>37</sup>N. D. Shrimpton, W. M. Cole, and W. A. Steele, in *Surface Properties of Layered Materials*, edited by G. Benedek (Kluwer, Dordrecht, 1991).  
<sup>38</sup>S. H. Suh, N. Lermer, and S. F. O'Shea, *Chem. Phys.* **129**, 273 (1989).  
<sup>39</sup>*Computer Studies of Phase Transitions and Critical Phenomena*, edited by O. G. Mouritsen (Springer-Verlag, Heidelberg, 1984).  
<sup>40</sup>*Applications of the Monte Carlo Method in Statistical Physics*, edited by K. Binder (Springer-Verlag, Heidelberg, 1979).  
<sup>41</sup>K. J. Strandburg, *Rev. Mod. Phys.* **60**, 161 (1988).  
<sup>42</sup>N. D. Shrimpton, H.-Y. Kim, W. A. Steele, and A. Cheng (unpublished).  
<sup>43</sup>S. N. Coppersmith, D. S. Fisher, B. I. Halperin, P. A. Lee, and W. F. Brinkman, *Phys. Rev. B* **25**, 349 (1982).  
<sup>44</sup>D. A. Huse and M. E. Fisher, *Phys. Rev. B* **29**, 239 (1984).